

14.0 CHARACTERIZATION OF REGIONS IN Ti-6Al-4V FORGINGS WITH DIMINISHED ULTRASONIC INSPECTABILITY

Connor Campbell (Mines)
 Faculty: Terry Lowe (Mines) and Kester Clarke (Mines)
 Industrial Mentor: Tony Yao (Weber Metals)

This project was initiated in Spring 2016 and is supported by CANFSA. The research performed during this project will serve as the basis for an M.S. thesis program for Connor Campbell.

14.1 Project Overview and Industrial Relevance

Titanium alloys are widely used in advanced structural applications due to their remarkable specific strength and corrosion resistance. The mechanical properties of two-phase alpha/beta titanium alloys, the most common of which is Ti-6Al-4V, depends strongly on the microstructure and texture developed during thermomechanical processing (TMP). Primary TMP of conventional alpha/beta alloys is typically conducted in multiple hot-working and heat treatment steps with the intent of ultimately achieving a uniform and fine-grained (UFG) microstructure of 15-20 μm equiaxed primary alpha (hcp) in a transformed matrix of alpha and beta (bcc) phase [14.1]. This microstructure is ideal because it suppresses the anisotropic properties of the alpha phase, promoting homogeneity of mechanical properties while increasing workability and ultrasonic inspectability [14.2]. The steps to produce this microstructure generally consist of hot working and heat treatment in the high-temperature single-phase beta field followed by breakdown of the transformed, lamellar microstructure in the lower-temperature two-phase alpha/beta field [14.1].

Localized heterogeneous deformation often arises during TMP of titanium alloys, particularly when deforming colonies of alpha lamellae. This is primarily due to the anisotropy and temperature-dependence of the critical resolved shear stress (CRSS) of various slip systems within alpha lamellae, which results in colonies being either hard- or soft-oriented with respect to the applied load depending on which slip systems are operational [14.3]. Previous work from Bieler and Semiatin has shown that in locations where both prismatic and basal slip systems are non-operational, shear bands develop that lead to kinked lamellar microstructural features. These shear bands allow localized shear to flow around hard regions, preventing hard colonies from dynamically recrystallizing into more equiaxed grains [14.4]. During ultrasonic testing, colony remnants can act as large elastic entities in an otherwise uniform and fine-grained microstructure, and may produce ultrasonic indications.

An ultrasonic pulse sent into a forging will scatter as it travels through the polycrystalline microstructure. This is due to the anisotropy of the elastic modulus in the alpha phase which correlates to the speed of sound within the grains. The extent of this scattering will vary depending on the relative size and orientation of the insonified grains and the wavelength and volume of the pulse. To inhibit noise, transducers are selected that produce pulses with wavelengths ($\lambda \approx 100\mu\text{m}$ for 10MHz transducers) greater than the average diameter ($D \approx 15\mu\text{m}$ for Ti-6Al-4V forgings) of the grains they travel through. This keeps the scattering within the Rayleigh regime ($\lambda > 2\pi D$), which has been shown to improve inspectability of near-alpha titanium forgings [14.5]. However, if alpha colony remnants are present ($D > 100\mu\text{m}$) they will shift the scattering into the stochastic regime ($\lambda < 2\pi D$), which can mask the presence of defects by increasing ultrasonic attenuation. For the above reasons, and many others not listed pertaining to quality control, the recrystallization of alpha colonies is of great interest to titanium producers.

14.2 Previous Work

This project is focused on experimentally observing microstructural heterogeneities in a Ti-6Al-4V forging that caused signals produced during ultrasonic testing (UT) to increase 3 to 4 times in certain areas. During routine ultrasonic inspection, indications were found at various locations within the forging. A section of the forging was then supplied by Weber Metals to Mines for further analysis.

14.3 Recent Progress

The following sections focus on work that has been completed since the last reporting period. Highlights include removal of regions of interest via wire electrical discharge machining (EDM), x-ray bulk texture analysis, and characterization of an alpha colony remnant and other non-ideal microstructures found in scanned regions identified as anomalous by UT inspection.

14.3.1 Scanning of Sample Material for Regions of Low Ultrasonic Quality

Sample material was supplied to Mines following beta-annealing and alpha-beta forging, but prior to alpha-beta heat treatment. The material was cut from a longer bar, with 5 regions identified with an immersed transducer and labeled with an engraving tool. The regions were labeled with percentages indicating the peak signal-to-noise ratio (SNR) produced during the scan relative to those produced by a 3/64" flat-bottom hole (FBH) standard. Regions 3 and 4 had typical SNRs equal to about 10% of those produced by FBH standards. However, regions 1, 2, and 5 produced signals 3-4 times stronger.

All scanned regions were extracted via wire EDM for analysis. Regions 1 and 2 were cut into rectangular prisms and prepared for acoustic inspection with a Sonix IC Inspection System. Regions 3, 4, and 5 were extracted as cylinders that were then cut to observe the microstructure along different planes of the forging. Cuts were made in region 5 to observe the microstructure above, below, and at the depth of the ultrasonic indication on a plane normal to the direction of ultrasonic inspection.

14.3.2 Characterization of Regions of Interest

The sample cut from region 5 at a depth of 2.38" (coin 2) was observed using a JEOL JSM 7000F field emission scanning electron microscope. Secondary electron images (SEI) were taken and electron backscatter diffraction (EBSD) maps were generated of an undeformed alpha colony in a location approximately below where the ultrasonic transducer was placed. The heterogeneity observed in this area is shown in **Figure 14.1**, and an inverse pole figure map of the area is overlaid in **Figure 14.2**. Though the boundaries of the colony are still apparent, the crystal orientations within the colony are sufficiently varied to indicate moderate deformation. Inverse pole figures were calculated using TSL/OIM software and the results are included in **Figure 14.3**, which show a fairly weak preferred orientation with a peak intensity of $\sim 2.4x$ random.

Samples taken from regions 1 and 2 at the depths of indications were also inspected in a similar fashion. In sample 1, there were no obvious heterogeneities like the alpha colony observed in **Figure 14.1**, but there were a notable lack of equiaxed alpha grains present. The grains were elongated, and this was even more noticeable in the sample taken from region 2. An example of the non-equiaxed microstructure is presented in **Figure 14.4**, detailing some coarse ($\sim 100\mu\text{m}$) alpha as well as elongated alpha grains that may be a result of localized plastic deformation. Larger grains have the potential to produce greater backscattering due to the shift in scattering mechanism from Rayleigh ($\lambda > 2\pi D$) to stochastic ($\lambda < 2\pi D$) scattering. Since these regions are near the surface of the part, it is possible that the material was deformed less due to thermal losses as well as die friction, perhaps resulting in less dynamic recrystallization.

14.4 Plans for Next Reporting Period

Further EBSD analysis will be performed of regions 1 and 2, and Taylor factor and slip transfer analysis will be performed using TSL/OIM software and MTEX in order to glean insight into how the colonies persisted throughout processing. Particular attention will be paid to deformation along the axial direction of the forging, and deformation at 30° and 45° rotations to the axis of the bar to determine how these alternate processing routes would impact slip within the colony remnants.

14.5 References

- [14.1] S. L. Semiatin, V. Seetharaman, I. Weiss. Flow behavior and globularization kinetics during hot working of Ti-6Al-4V with a colony alpha microstructure. *Materials Science and Engineering A*. 263 (1999) 257-271.
- [14.2] X. Ma, W. Zeng, F. Tian, Y. Zhou. The kinetics of dynamic globularization during hot working of a two phase titanium alloy with starting lamellar microstructure. *Materials Science and Engineering A*. 548 (2012) 6-11.
- [14.3] S. L. Semiatin, T. R. Bieler. Effect of texture and slip mode on the anisotropy of plastic flow and flow softening during hot working of Ti-6Al-4V. *Metallurgical and Materials Transactions A*. 32A (2001) 1787-1799.
- [14.4] S. Roy, S. Suwas. Orientation dependent spheroidization response and macro-zone formation during sub-beta transus processing of Ti-6Al-4V alloy. *Acta Materialia* 134 (2017) 283-201.

- [14.5] M. Gigliotti, B. Belway, J. Deaton et al. Microstructure-ultrasonic inspectability relationships in Ti6242: signal-to-noise in fine-grain-processes Ti6242. Metallurgical and Materials Transactions A. 31A (2000) 2119-2125.

14.6 Figures

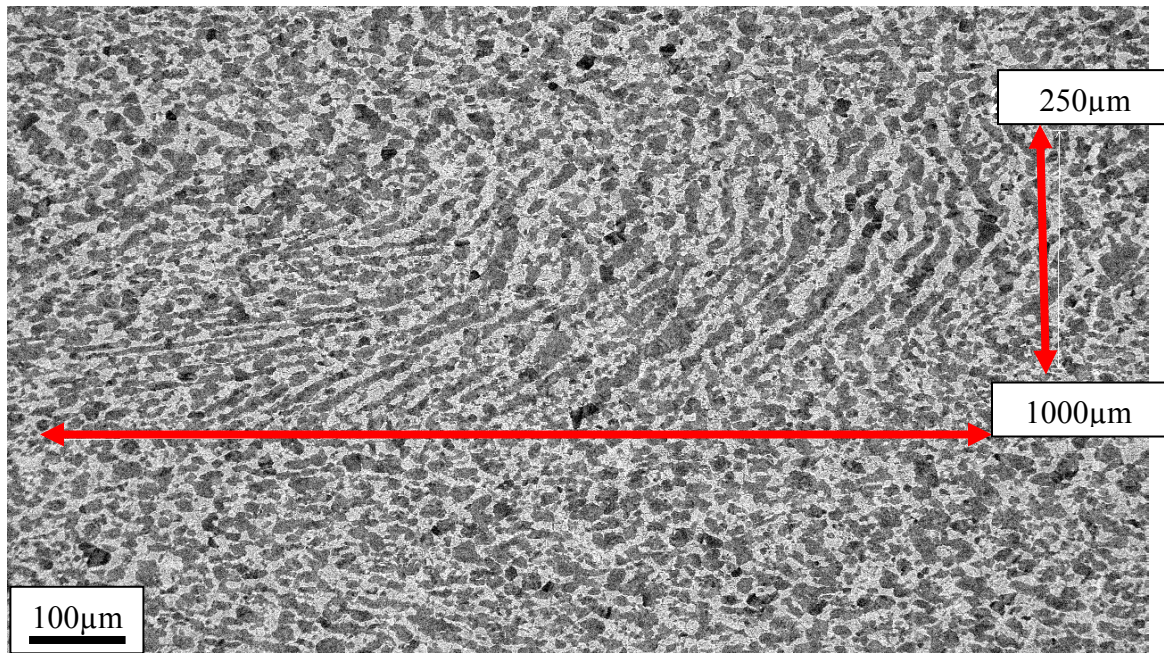


Figure 14.1: SEM-BEI image taken from Sample 5 at a location approximately below the transducer location at the depth of the indicated flaw. The pictured heterogeneity was mapped via electron backscatter diffraction for crystallographic orientation in order to determine extent of preferred orientation and the resulting dataset can be analyzed for ultrasonic interactions.

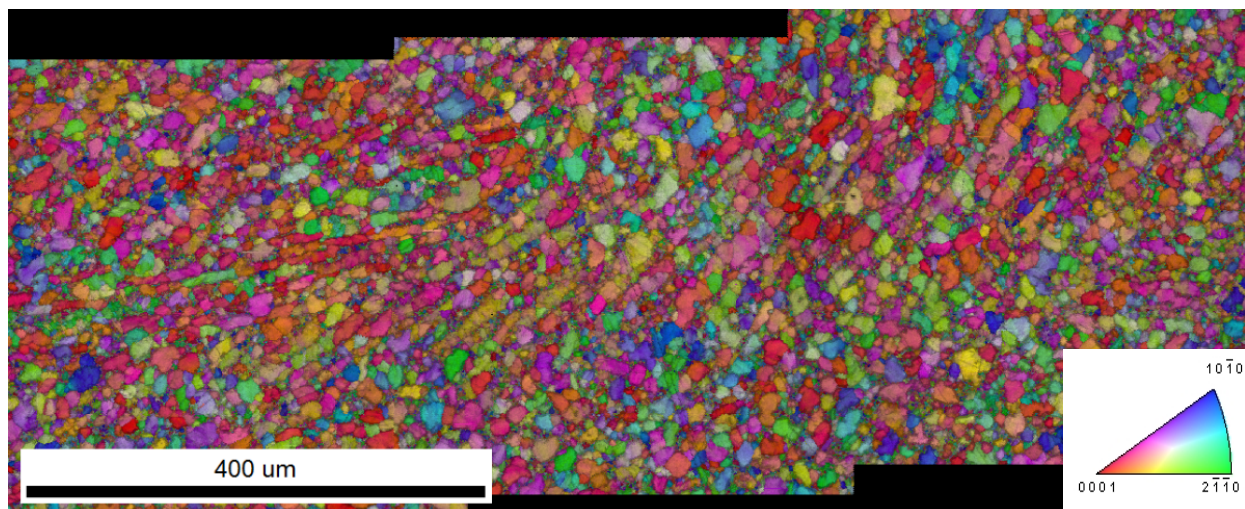


Figure 14.2: SEM-BSE image taken from Sample 5 with an electron backscatter diffraction orientation map overlaid. Multiple EBSD scans were stitched to form a single dataset, from which local texture and grain size distribution can be calculated. EBSD courtesy of B. Terry at Mines.

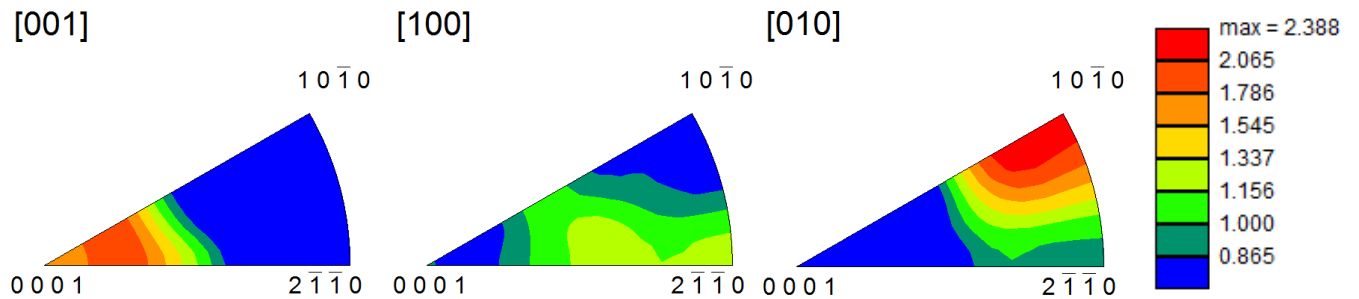


Figure 14.3: Inverse pole figure texture intensities calculated using TSL/OIM software from the EBSD map in **Figure 14.2**. The maximum intensity of 2.388 times random is on the low end of intensities that would cause ultrasonic scattering at the levels measured, which warrants further analysis.

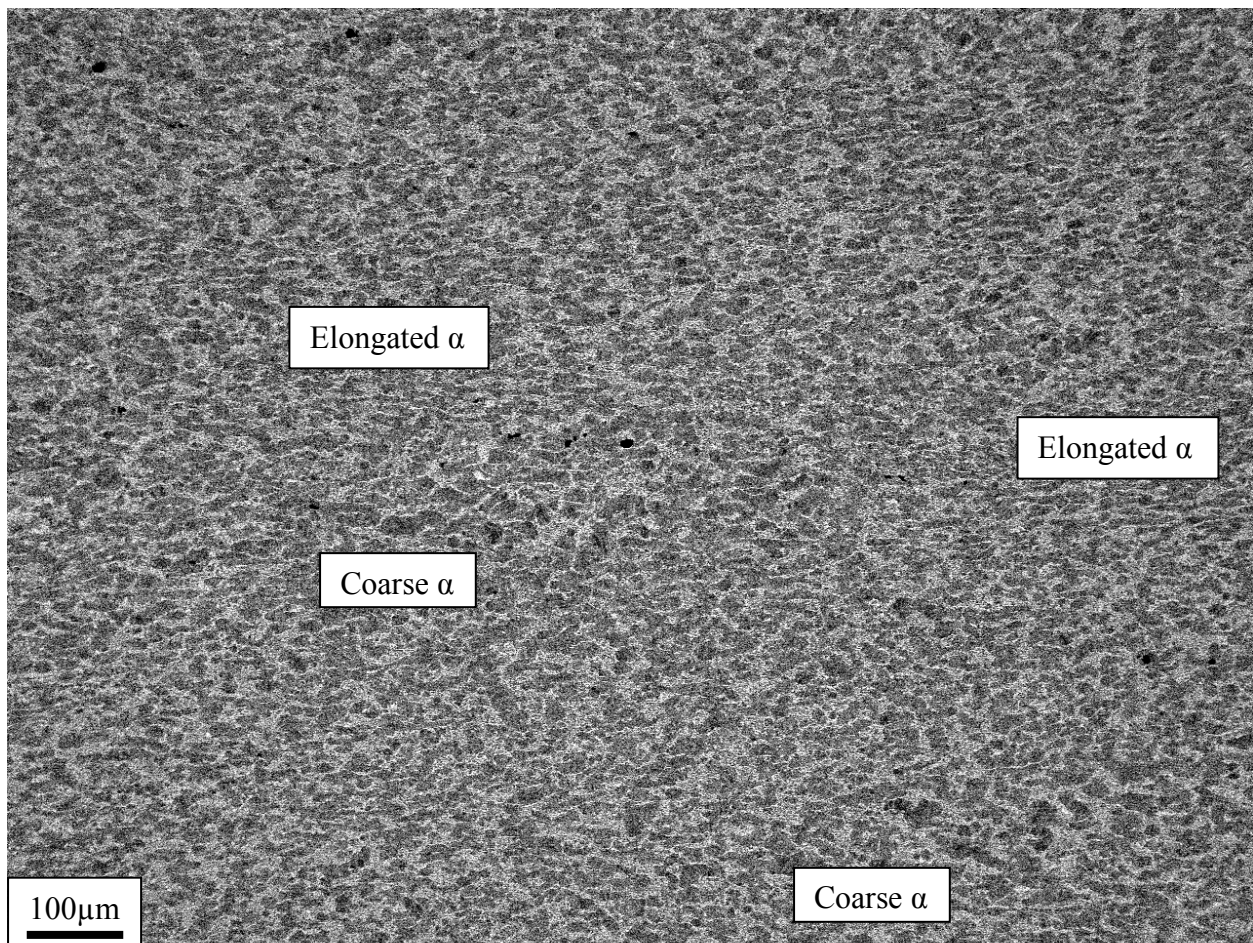


Figure 14.4: Coarse (~100µm) alpha grains found near a region of heavily-deformed and elongated alpha grains that provides evidence of heterogeneous plastic deformation. The heavily recrystallized region above and below the coarse region and the presence of highly elongated grains may indicate plastic deformation flowing around a hard-oriented alpha colony. EBSD analysis will provide further insight.